

Effect of active metal coatings on the mechanical properties of silicon nitride-based ceramics

S. KANG*, J. H. SELVERIAN†

GTE Laboratories Incorporated, 40 Sylvan Road, Waltham, MA 02254, USA

The effects of titanium, zirconium, hafnium and tantalum coatings on the mechanical properties of three silicon nitride ceramics were studied. The titanium coatings was found to cause a 50% decrease in the four-point bend strength of one of the silicon nitride ceramics while the effects of the zirconium, hafnium and tantalum coatings on all three silicon nitride ceramics were moderate. The reactions at a high temperature (940–980 °C) between titanium and the grain-boundary glassy phase was the major cause for the degradation of the ceramic properties by the titanium coating. Residual tensile stress developed at the reaction interface replaced the glassy grain-boundary phase. Analytical electron microscopy showed the formation of a 180 nm thick Ti_5Si_3 layer and the crystallization of the amorphous grain-boundary phase. An indentation technique was used to measure qualitatively the residual stress developed at the reaction interface.

1. Introduction

Silicon nitride ceramics have an attractive set of properties which make them useful structural materials. These properties include high strength at room and elevated temperatures, excellent corrosion and wear resistance, and low thermal expansion with moderate elastic modulus, which result in minimal stress during thermal transients [1].

The ability to be joined to other materials, particularly metals, is essential for structural ceramics to attain widespread application. Brazing is often the preferred method for joining ceramics to metals because it can provide hermetic seals and because the plasticity of the braze accommodates the differential expansion between the ceramic and metal. Braze alloys which readily wet and bond to metals do not usually wet ceramics without the presence of an active metal coating. Active metal coatings react with the ceramic to promote good wetting by braze alloys and to enhance the adhesive strength between the braze and ceramic. Despite the relatively common use of the active metal coatings, little is known about the effect of their interactions with silicon nitride ceramics on joint performance.

Among various active metal coatings, titanium is the most widely used for ceramic bonding. Titanium was reported [2–5] to react extensively with silicon nitride, forming TiN and titanium silicides at or above 800 °C. Based on these earlier works, the TiN and $TiSi_2$ phases are presumed to be present at the interface in titanium-coated Si_3N_4 -based ceramics used in this

study. Other coating materials such as tantalum, hafnium and zirconium also tend to form nitride phases when they react with a silicon nitride substrate. However, ZrN and HfN start forming at much higher temperature than TiN [6] even if these have a strong tendency to form thermodynamically. The TaN phase was observed to form at 1500 °C with other silicides (Ta_3Si_3 and $TaSi_2$).

In the course of ceramic–metal joint development by using titanium coating, it was important to understand the effect of reactions between titanium and silicon nitride ceramics on the mechanical properties of silicon nitride, and the nature of the reactions between the active metal and the grain-boundary phase. In order to address these issues, three silicon nitride ceramics with different contents of Y_2O_3 and Al_2O_3 were chosen for study. These were AY6 (Si_3N_4 –6% Y_2O_3 –1.5% Al_2O_3), SNW1000 (Si_3N_4 –13% Y_2O_3 –1.5% Al_2O_3), and PY6 (Si_3N_4 –6% Y_2O_3), (all produced by WESGO, Belmont, CA 94002; all compositions weight per cent). In this work, the effects of active metal coatings on the mechanical properties of three silicon nitride ceramics were quantified. Also, a mechanism for the reduction in modulus of rupture in four-point bending (MOR) strength of silicon nitride caused by titanium coatings is suggested on the basis of residual stress measurements and the microstructure of the coating/ceramic interface. Other active coatings such as zirconium, hafnium and tantalum were used to compare their impacts on the mechanical properties of the ceramics with that of titanium.

* Present address: Valenite Inc., 1711 Thunderbird St., Troy, MI, 48084, USA.

† Present address: Osram Sylvania Inc., 60 Boston St., Salem, MA, 01970, USA.

2. Experimental procedure

2.1. Sample preparation

The AY6, SNW1000, and PY6 MOR bars, were polished to an optical grade finish with 0.03 μm alumina powder. Active metal coatings were deposited on one side of each sample by electron-beam evaporation at 300 $^{\circ}\text{C}$ in a 10^{-3} Pa vacuum. The coatings were 3 μm thick for mechanical testing and 0.1 μm thick for Auger analysis.

A glass phase, simulating the grain-boundary composition of the AY6, was produced to study reactions between titanium and the bulk grain-boundary phase. A powder mixture of Y_2O_3 -26.9% SiO_2 -16.7% Al_2O_3 -5.8% Si_3N_4 (wt %) was melted in a molybdenum crucible at 1700–1850 $^{\circ}\text{C}$ in a nitrogen atmosphere to make the simulated AY6 grain-boundary phase as elsewhere [7]. The glass was polished to an optical grade as done for silicon nitride ceramics, and coated with titanium. The effect of the titanium coating was studied on the interface microstructure and the size of indentation cracks.

2.2. Mechanical testing

The effects of reactive coatings on the mechanical properties of the ceramics were evaluated with MOR strength tests in four-point bending. MOR bars (25.4 mm \times 2.5 mm \times 1.27 mm) were machined from four or five different ceramic blanks to obtain sampling of average ceramic strengths. MOR bars from a given ceramic blank were distributed among the different tests. All of the MOR bars were coated at the same time for each coating material. Coated MOR bars of SNW1000, AY6 and PY6 were held at 940–980 $^{\circ}\text{C}$ for 7–10 min in a vacuum of 10^{-3} Pa. These heat treatments simulated a typical brazing cycle for these materials. MOR testing was performed at room temperature using a hydraulic testing machine and a strain rate of 0.05 cm min^{-1} with the coated side of the MOR bar in tension. The inner span of the four point bending apparatus was 10 mm and the outer span was 23 mm.

Crack sizes from microhardness indentations in both titanium-coated AY6 glass samples and uncoated AY6 glass samples were measured using a Tukon microhardness tester. Titanium-coated AY6 glass samples were heated under the same conditions as for silicon nitride bars and polished with 6, 3, and 1 μm diamond pastes at a 5–10 $^{\circ}$ angle until the reaction layer was just exposed. Indentations were made along the edge of the titanium-coating layer and the crack size was measured as a function of applied load. The uncoated samples were heat-treated and polished in the same way to provide a valid comparison for the effect of the coating.

2.3. Microstructure

Cross-sectional samples of the titanium-coated glass were prepared for transmission electron microscopy study. Two bars were glued together with the coated sides facing each other, using a high-temperature epoxy. Samples were obtained by core-drilling and dimpled down to a thickness of 10 μm . The samples

were ion-milled to perforation with 4–5 keV Ar^+ ions at an incident beam angle of 15 $^{\circ}$. Analytical TEM was performed with a Philips EM 400T operating at 120 keV. The reaction product between the titanium coating and the glass was identified by electron energy loss and electron diffraction analysis.

3. Results

The effects of various coatings on the MOR strength of AY6, SNW1000, and PY6 are summarized in Table I. Sintered and hot isostatically pressed AY6 exhibited an extremely high room-temperature MOR strength (\sim 1350 MPa). However, as shown in the table, the titanium coating, heat treated at 940–980 $^{\circ}\text{C}$ for 7–10 min, caused a 45% reduction in average MOR strength compared to as-polished and vacuum heat-treated AY6. Tantalum coatings caused a 12% decrease in the MOR strength of AY6, while zirconium and hafnium did not cause any significant reductions in the MOR strength of AY6. For SNW1000, heat treatment of the titanium-coated bars caused a \sim 20% reduction in the average MOR strength, while heat-treatment of the hafnium- or zirconium-coated bars caused less than 10% reduction in the average MOR strength, compared to as-polished SNW1000 bars. In contrast with the large reduction in the MOR strength of AY6, the titanium-coating caused minimal decrease in the MOR strength of PY6. PY6 with titanium coatings exhibited a 5% reduction in the MOR strength after heat treatment. The Weibull moduli of the titanium- or zirconium-coated AY6 were increased compared to that of uncoated AY6. The Weibull modulus of PY6 was not sensitive to the presence of any coatings. The effect of tantalum on the MOR strength was not fully assessed due to the poor adhesion of the coating to the ceramic substrate after heat treatments.

TABLE I Average strength and standard deviation from four-point MOR tests of titanium-, zirconium-, hafnium- and tantalum-coated AY6, SNW1000, and PY6 silicon nitride ceramics. All samples were vacuum annealed at 940–980 $^{\circ}\text{C}$ for 7–10 min prior to testing. An analysis of variance (ANOVA) test was used to decide whether the difference between the coated and uncoated bars was significant at the 95% level

Sample	Average MOR (MPa)	Standard deviation (MPa)	Is difference significant ^a (% difference)
Uncoated AY6	1338	51	–
Ti/AY6	740	9	y (45%)
Zr/AY6	1327	37	n
Hf/AY6	1267	47	n
Ta/AY6	1173	34	y (12%)
Uncoated SNW1000	533	12	–
Ti/SNW1000	429	18	y (20%)
Zr/SNW1000	478	27	n
Hf/SNW1000	509	16	n
Ta/SNW1000	475	17	y (10%)
Uncoated PY6	763	19	–
Ti/PY6	729	15	n (5%)
Zr/PY6	734	26	n
Hf/PY6	731	15	n
Ta/PY6	769	13	n

^a y = yes, n = no.

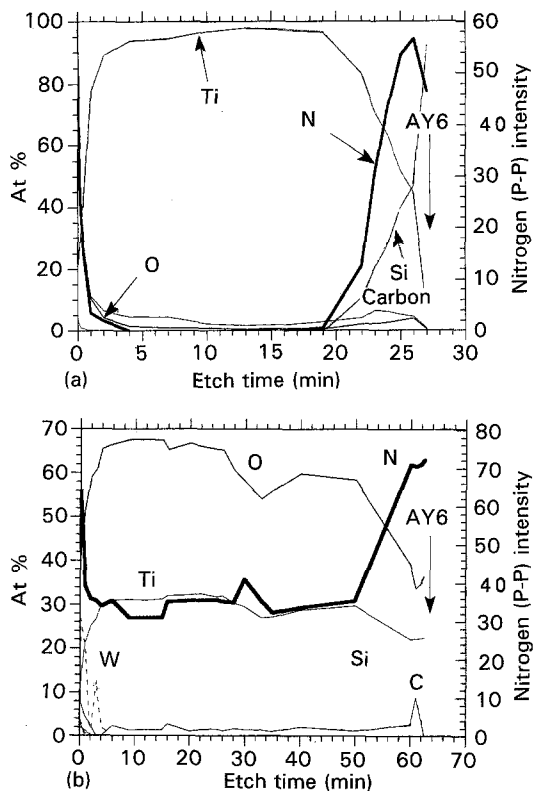


Figure 1 Auger profiles of the titanium-coated AY6: (a) as-deposited, and (b) annealed in vacuum at 940 °C for 7 min. Note that most of the TiO_2 forms during heat treatment.

Auger depth profiles from the titanium-coated (0.1 μm) AY6 samples are shown in Fig. 1. Fig. 1a represents the surface condition of the as-deposited sample before heat treatment. Oxygen contamination was found to be insignificant during the coating process. In contrast, a significant amount of oxygen was found in the titanium layer during the heat-treatment in a 10^{-3} Pa vacuum, Fig. 1b. The ratio of titanium to oxygen was about 1:2, indicating TiO_2 formation. A similar atomic per cent for titanium and nitrogen indicated the formation of TiN . Owing to the nature of this analysis, the presence of silicides between titanium and silicon nitride was not confirmed.

Scanning electron microscopy was performed to find the effect of the titanium-coating on the fracture behaviour of the MOR bars. AY6 silicon nitride was selected for the study of interface microstructure due to its drastic loss of MOR strength after titanium/substrate reactions. As shown in Fig. 2, the fracture origins were often associated with impurities, voids, or surface flaws and the presence of titanium coating did not produce noticeable changes in general fracture morphology. It is common to see fractures of MOR bars originated from impurities or surface flaws in silicon nitride materials. Based on the SEM and MOR testing results, it can be said at least that the threshold stress for crack initiation in the vicinity of impurities was reduced significantly by the reaction of titanium coating with the silicon nitride on the tension side of an MOR bar.

Extensive transmission electron microscopy was also carried out to investigate the reaction zone. However, the fine-grain (boundary) structure of AY6

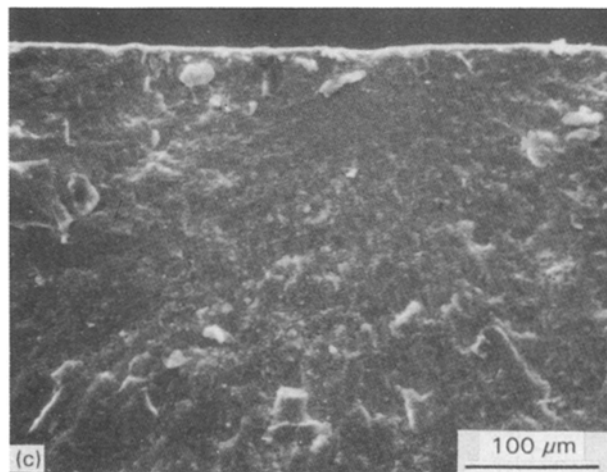
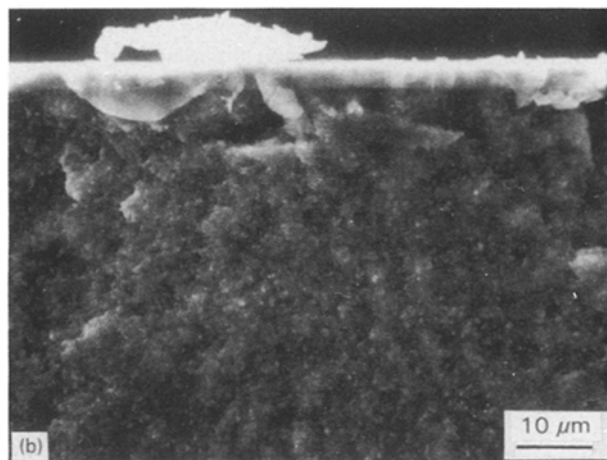
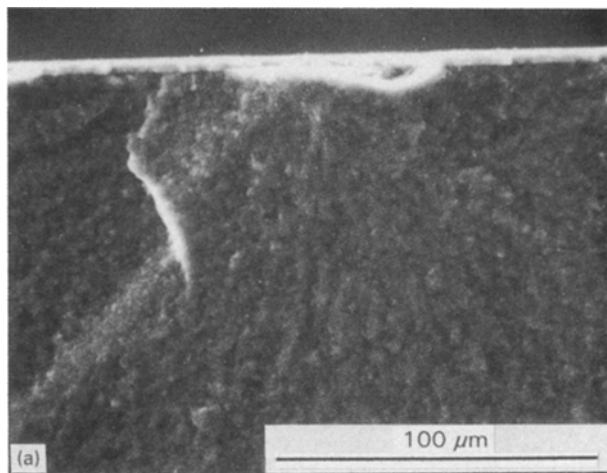


Figure 2 Fracture origins of titanium-coated MOR bars: (a) surface flaw, (b) void, and (c) no apparent origin.

silicon nitride ($< 2 \mu\text{m}$ in grain size) made the direct observation of the interfacial reaction zone extremely difficult with an electron microscope unless a large pool of grain-boundary phase like in triple points exposed to the titanium coating could be found. Because such a large pool of grain-boundary phase was not seen in contact with the titanium-coating, AY6 glass which simulated the grain-boundary phase of AY6 silicon nitride, was used to illustrate the reaction and its effect on the strength reduction. Fig. 3 shows a transmission electron micrograph of a Ti/AY6 glass interface. It shows the formation of a discrete phase

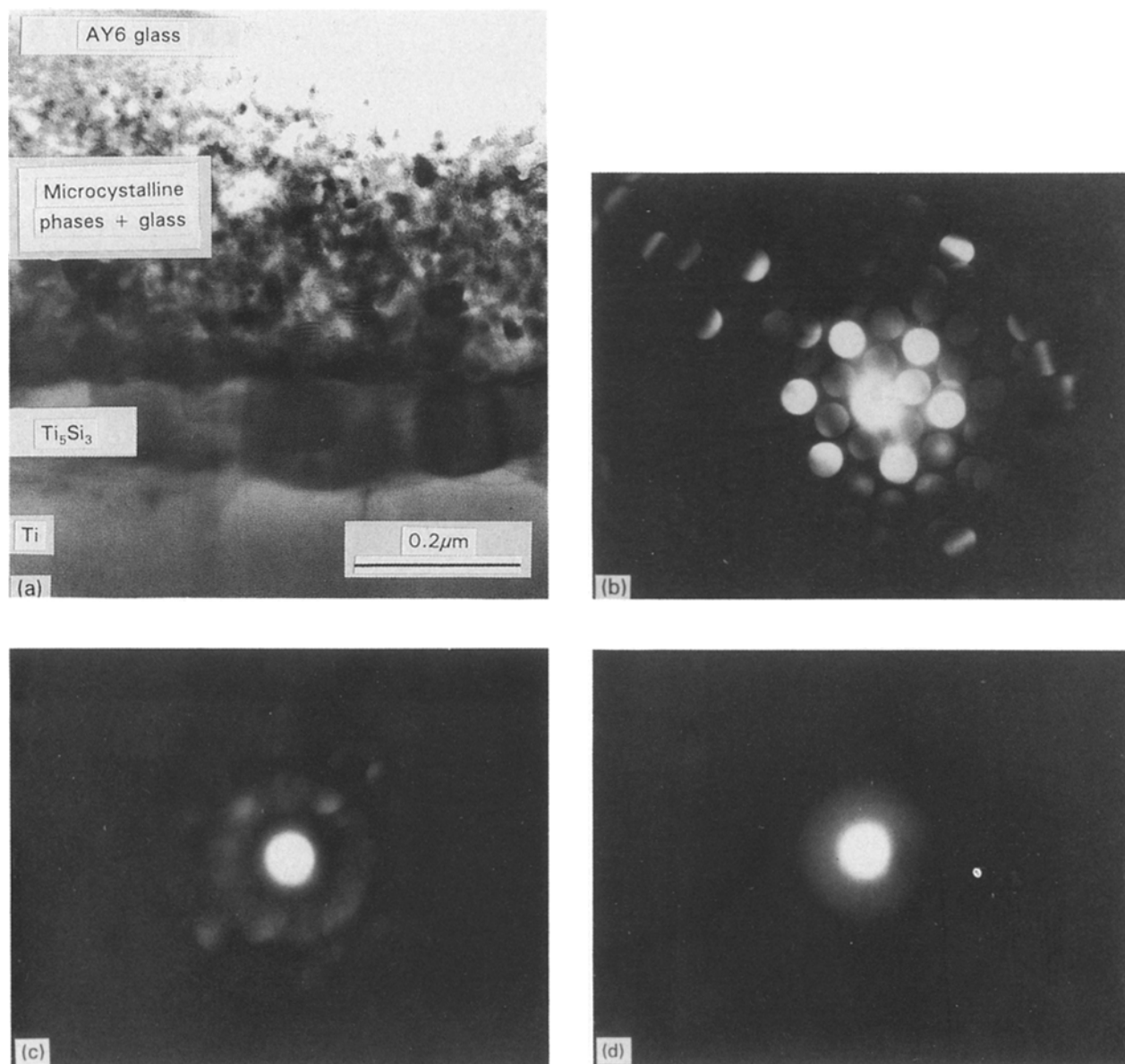


Figure 3 Transmission electron micrographs of the interface between titanium and AY6 glass: (a) bright-field micrograph, (b) diffraction pattern of Ti_5Si_3 , (c) diffraction pattern from the microcrystalline + glass region, and (d) diffraction pattern from the glass region.

at the interface and microcrystalline phases that appeared to begin forming near the interface. The discrete phase was identified as Ti_5Si_3 by a convergent-beam electron diffraction and energy dispersive X-ray analysis (EDXA). The formation of these phases along the Ti/AY6 glass interface was uniform in morphology and size: 100–180 and 10–60 nm for the Ti_5Si_3 and microcrystalline phase, respectively. Ti_5Si_3 seemed to be coherent with the titanium layer and the surrounding microcrystalline phase.

Diffraction patterns in Fig. 3b–d show the transition of the interface region from the Ti_5Si_3 phase to AY6 glass. The microcrystalline phase was not identified due to the size. The compositions of the microcrystalline + glass region and the AY6 glass composition were found to be similar to one another within the accuracy of EDXA.

To aid in understanding the effect of new phases on the mechanical properties of AY6 silicon nitride, the level of residual stress at the Ti/AY6 glass interface was measured, using an indentation technique

suggested by Marshall and Lawn [8]. The indentation measurements were performed on the titanium-coated AY6 silicon nitride. The measurements were not sensitive enough to reflect the effect of reaction products obtained from short-time reaction (7–10 min) at 980 °C. This can be expected due to the small volume fraction of the grain-boundary phase and the coarse nature of the measurement. Therefore, the samples were made of 100% AY6 grain-boundary phase material. The relationship between the residual stress and crack size was given as

$$\left(\frac{P}{c^{3/2}}\right)_{\sigma_R} = \left(\frac{P}{c^{3/2}}\right)_0 \left(1 + \frac{2m\sigma_R c^{1/2}}{K_c \pi^{1/2}}\right) \quad (1)$$

where P is the indentation load, c the crack length, $(P/c^{3/2})_0$ a constant defined for the stress-free sample, σ_R the residual stress, K_c a material parameter, and m a dimensionless modification factor; $m = 1$ when free-surface effects and stress gradients over the depth of the crack are neglected [9]. A linear plot of $(P/c^{3/2})$ versus $c^{1/2}$ would give σ_R i.e. the level of residual stress

for the titanium-coated and uncoated samples, for comparison. Fig. 4 illustrates the results obtained from the coated and uncoated glass materials. In spite of the non-linearity of the plots, a relative comparison can be made in terms of the slopes of the curves for a

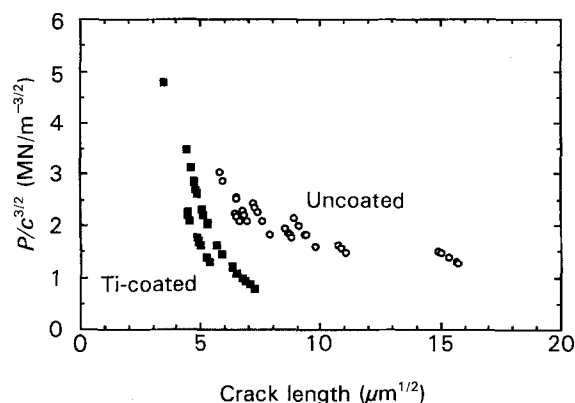


Figure 4 A plot ($P/c^{3/2}$) versus $c^{1/2}$; the level of residual stress can be obtained from the slope of the curves. Titanium-coated samples showed two to three times higher residual stress than that of uncoated samples.

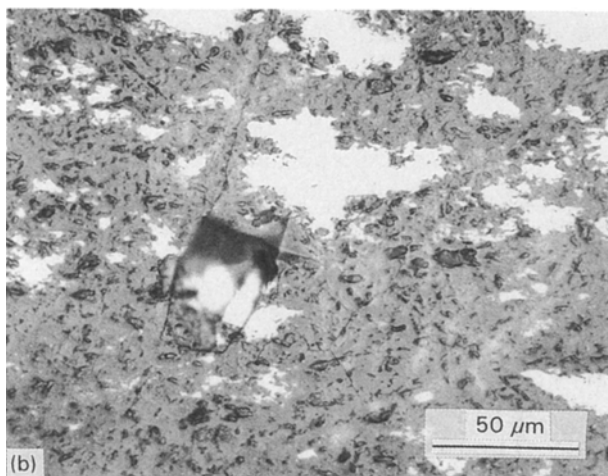
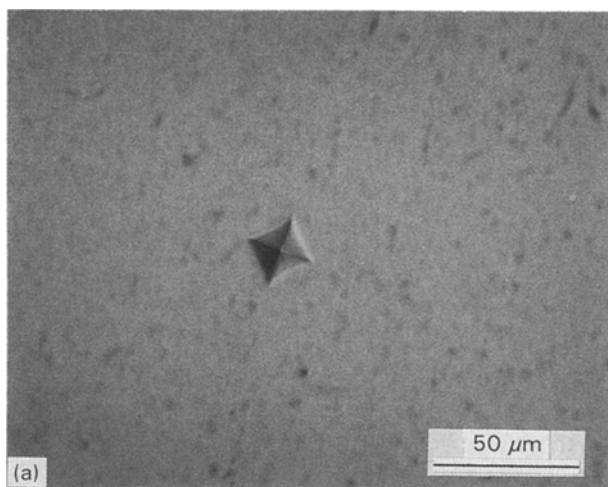


Figure 5 (a) Uncoated AY6 glass indented with a 300 g load. The glass surrounding the indent did not crack. (b) Titanium-coated glass indented with a 300 g load. The glass surrounding the indent cracked and spalled. This indicated that the glass had large tensile stresses at the surface.

given crack size. Non-linear behaviour of Fig. 4 was attributed to the modification factor, m , which was expected to become a complex diminishing function of c in the area where the stress gradient was high [8]. As noted from the slopes of the curves, the titanium-coated glass (steep slope) retained significantly higher residual tensile stress on the surface compared to the case of uncoated glass (shallow slope). The ratio of the slopes indicated that titanium/glass interactions increased the level of the residual stress by a factor of 2–3 compared with uncoated samples, assuming that the modification factor, m , was the same in the coated and uncoated samples at a given crack size. An indent made on the uncoated AY6 glass with a 300 g load did not crack the surrounding glass, Fig. 5a. In contrast, the indent made on the titanium-coated glass surface with a 300 g load resulted in extensive cracking and shattered the surface, Fig. 5b.

4. Discussion

The MOR results in Table I showed that active metal coatings degraded the mechanical properties of the silicon nitride ceramics even after short-time heat treatment at high temperature. In addition, heated, uncoated MOR bars did not show any strength degradation. It was found from a separate study that the strength values of titanium-coated MOR bars, which were not heat treated, were at least equivalent to, or slightly higher than, those obtained from as-polished bars [6]. A stable or non-reactive coating layer on the ceramic bar might increase the MOR strength of the silicon nitride by blunting the surface flaws on ceramics. Thus, it can be said that the reactions between active metal coatings and the silicon nitride caused the MOR strength degradation.

The degree of reduction in MOR strength depended on coating materials and ceramic substrates. The titanium-coatings decreased the MOR strength the most, while zirconium, tantalum and hafnium coatings did not degrade the strength appreciably. The interactions between active coating materials and the grain-boundary phase were considered as a potential cause of the differences in the reduction of the MOR strength. AY6, SNW1000, and PY6 contain different amounts of Al_2O_3 and Y_2O_3 as sintering aids. It is known that the relative amount of Al_2O_3 and Y_2O_3 determines the degree of crystallinity of the grain-boundary phase [7]. The grain-boundary phases were composed of Al_2O_3 , Y_2O_3 , Si_3N_4 , and SiO_2 . The SiO_2 arises from an oxygen-rich surface layer on the starting silicon nitride powders, probably from the oxidation of silicon nitride during milling. A small amount of silicon nitride exists in the grain-boundary phase which is dissolved from the surrounding silicon nitride grains. PY6, which does not have Al_2O_3 as a sintering aid, has a grain-boundary phase of predominantly crystalline $Y_2Si_2O_7$ [7]. Table II lists the ratio of Al_2O_3 to Y_2O_3 , the identity of the grain-boundary phases, and the decrease in the MOR strength of AY6, SNW1000, and PY6 ceramics. The reduction in the MOR strength increased with a decrease in the Y_2O_3 to Al_2O_3 ratio.

TABLE II Bulk compositions, grain-boundary phases, and reduction in MOR strength due to titanium coating for the three silicon nitride ceramics studied. As the content of the amorphous phase increased in these silicon nitrides, the reduction in the average MOR strength increased

Ceramic	Composition (wt %)			Y ₂ O ₃ /Al ₂ O ₃ wt. ratio	Grain-boundary phases	Reduction in average MOR strength (%)
	Y ₂ O ₃	Al ₂ O ₃	Si ₃ N ₄			
AY6	6	1.5	bal.	4	Y ₂ O ₃ -Al ₂ O ₃ -SiO ₂ -Si ₃ N ₄ (amorphous)	45
SNW1000	13	1.5	bal.	8.7	Y ₂ O ₃ -Al ₂ O ₃ -SiO ₂ -Si ₃ N ₄ (amorphous)	20
PY6	6	-	bal.	∞	Y ₂ Si ₂ O ₇ 10Y ₂ O ₃ ·9SiO ₂ ·Si ₃ N ₄	5

The suggested mechanism of strength degradation for the titanium-coated silicon nitrides is that titanium readily forms new phases at the grain boundaries, or causes the devitrification of the grain-boundary phase in AY6 and SNW1000. It was reported [10–13] that TiO₂ and ZrO₂ were used as grain-boundary phase nucleating agents to improve the high-temperature properties of some silicon nitride ceramics by forming crystalline phases. Titanium might serve a similar role by forming TiO₂ in the grain-boundary phase. ZrO₂ was found to induce a greater degree of crystallization than TiO₂ at higher temperatures. TiO₂ was presumed to have a lower activation energy for crystallization than ZrO₂ at temperatures below 1300 °C, while ZrO₂ becomes more active as temperature increases [6, 14]. This was supported by the fact that zirconium coating reduced the MOR strength at higher temperature (1300 °C) significantly in a separate experiment.

New phase formation at the interface between titanium coating and the glass phase, Fig. 3, or precipitation of a crystalline phase in the grain-boundary phase induces significant residual stress between the crystalline phase and the surroundings [15]. Residual tensile forces would be induced at the interface between new phase(s) and the surrounding glass in the grain-boundary region if a portion of the amorphous grain-boundary phase were replaced by a crystalline phase with a higher density (see Fig. 4). Thus, the interface becomes more susceptible to cracking. In support of this conclusion it has been reported that the volume change associated with the polymorphic inversion of Y₂Si₂O₇ in a Y₂O₃-SiO₂ system was as large as 6.7% [16] and a high dislocation density formed in the silicon nitride grains upon crystallization [17]. Further, the presence of the TiO₂/(Ti)/Ti₅Si₃ layer on top of the microcrystalline phase enhances crack initiation or propagation due to the thermal expansion mismatch between the layer and glassy grain-boundary phase. A study with titanium-coated sapphire [18] showed that the level of stress developed at the interface between sapphire and the reaction phase, Ti₃Al, was in the range of 650 MPa and the presence of this layer reduced the MOR strength by 60%.

Figs 4 and 5 demonstrate the presence of residual stress at the reaction in the AY6 glass material. This result can be extended to say that the degradation of the MOR strength of AY6, SNW1000, and PY6

silicon nitride was assisted by the residual tensile stress built-up in the grain boundaries which were in contact with the titanium-coating layer. This type of reaction between titanium and an amorphous grain-boundary phase is expected to be a general phenomenon. The investigations on titanium-coated Al₂O₃ ceramics have shown the same results as reported here [18]. This study showed strain contours near the Ti₅Si₃ phase which formed between titanium coating and a silicate glass in the grain boundary. Also, precipitation of a new phase was observed in the grain boundary of 99.5% alumina beneath the titanium-coating layer. Various polycrystalline aluminas with titanium coating exhibited a 15%–25% MOR strength reduction compared to uncoated counterparts. This study calculated the level of stress developed between the alumina substrate and an adjacent phase, Ti₃Al, also, formed due to the reaction.

Some other factors such as oxygen contamination of the titanium-coating layer and interaction between titanium and silicon nitride grains were also considered. However, because these factors would influence all three silicon nitrides to the same extent, the reduction in the MOR strength of the three silicon nitrides should be similar. Specifically, titanium-coated PY6 did not exhibit a noticeable reduction in strength compared to AY6, implying that the reaction between coating materials and silicon nitride grains has a minor effect on the MOR property degradation. Auger analysis in Fig. 1b showed that TiO₂ formed on the silicon nitride surface. The formation of new phases, i.e. TiO_x, TiN, or various silicides, or a phase transformation at a planar interface could cause changes in mechanical behaviour of the coated silicon nitride due to volume changes, strain mismatch, and/or thermal expansion mismatch. Transitions of silicides that formed at the Ti/Si₃N₄ interface from Ti₅Si₃ to TiSi₂ were seen. All the combined effects of the reaction between titanium and silicon nitride grains and the oxidation of the titanium-layer did not change the MOR strength of the silicon nitrides by more than 5%, based on the titanium-coated PY6 results. Therefore, these factors were ruled out as major causes for the degradation effect.

5. Conclusions

The primary purpose of active metal coatings such as titanium, zirconium, hafnium and tantalum in

ceramic-to-metal joining is to achieve better bond strength by promoting wetting of the ceramic substrate by the braze alloy. However, strong reactions between coatings and ceramic materials can cause deleterious effects on the strength of the ceramic. The most significant reduction in MOR strength was observed from the titanium-coated silicon nitrides which have a higher content of grain-boundary glass phase than others.

Among the factors responsible for the degradation of the ceramic properties by the titanium coating, the reactions between titanium and the grain-boundary glassy phase was the major cause. Titanium interacted with the grain-boundary phase, forming Ti_5Si_3 and a microcrystalline phase at the interface region. An indentation technique showed that the formations of Ti_5Si_3 and microcrystalline phases near the interface caused the grain-boundary region to be highly susceptible to cracking. This cracking was facilitated by the residual stress developed at the interface between new phases and existing grain-boundary phase. The volume change accompanied by the formation of microcrystalline phase and thermal mismatch between Ti_5Si_3 and grain-boundary phase resulted in two to three times higher residual tensile stress at the interface compared to the uncoated sample.

Based on these results, degradation of the mechanical properties of some structural ceramic materials may preclude the use of reactive metals such as titanium as a coating material where tensile forces will be applied. The effects of active coating materials on the mechanical properties of a ceramic are closely related to variables such as reaction temperature, time, and contents of amorphous phases in the system.

Acknowledgements

The authors thank H. J. Kim and M. L. Santella for their continuous interest and encouragement, D. Bazinet and G. McCloud for experimental assistance and useful discussion, and G. Baldoni, A. Pasto and W. Rhodes for manuscript reading and suggestions. DOE funding for the programme through Oak Ridge National Laboratory (Contract DE-AC05-84OR21400) is gratefully acknowledged. The authors

also acknowledge the contribution of C. Sung, K. Ostreicher, and M. Downey, Materials Characterization Department, for their assistance in analytical electron microscopy and X-ray analysis.

References

1. F. F. LANGE, *Int. Met. Rev.* **25** (1980) 1
2. I. BARIN and O. KNACKE, "Thermodynamic Properties of Inorganic Substances" (Springer, Berlin, 1973) p. 789.
3. R. BEYERS and R. SINCLAIR, *J. Vac. Sci. Technol.* **B2** (1984) 781.
4. A. E. MORGAN, E. K. BROADBENT and D. K. SANDANA, *Appl. Phys. Lett.* **49** (1986) 1236.
5. J. C. BARBOUR, A. E. T. KUIPER, M. F. C. WILLEMSEN and A. H. READER, *Appl. Phys. Lett.* **50** (1987) 953.
6. S. KANG, E. M. DUNN, J. H. SELVERIAN and H. J. KIM, *Am. Ceram. Soc. Bull.* **68** (1989) 1608.
7. J. T. SMITH and C. L. QUACKENBUSH, *ibid.* **59** (1980) 529.
8. D. B. MARSHALL and B. R. LAWN, *J. Am. Ceram. Soc.* **60** (1977) 86.
9. A. S. KOBAYASHI, "Experimental Techniques in Fracture Mechanics", edited by A. S. Kobayashi (Ohio State University Press, Ames, IA, 1973) p. 4.
10. W. BRAUE, G. WOTTING and G. ZIEGLER, in "Proceedings of the 2nd International Symposium on Ceramic Materials and Composites for Engine", Lubbeck-Travemunde, FRG, 14-17 April 1986, edited by W. Bunk and H. Housner (Verlag Deutsche Keramische Gesellschaft, 1986) p. 503.
11. P. E. DOHERTY, D. W. LEE, and R. S. DAVIS, *J. Am. Ceram. Soc.* **50** (1967) 77.
12. G. H. BEALL and D. A. DUKE, *J. Mater. Sci.* **4** (1969) 340.
13. G. H. BEALL, B. R. KARSTETTER and H. L. RITTLER, *J. Am. Ceram. Soc.* **50** (1967) 181.
14. D. R. STEWART, in "Advances in Nucleation and Crystallization in Glasses", edited by L. L. Hench and S. W. Freiman, Proceedings of the Symposium of the Glass Division of the American Ceramic Society, 26-28 April, 1971 (American Ceramic Society, OH, 1971) p. 26.
15. G. E. HILMAS and W. E. LEE, in "Proceedings of the 46th Annual Meeting of the Electron Microscopy Society of America", San Francisco, CA, edited by G. W. Bailey, (San Francisco Press Inc., San Francisco, CA, 1988) p. 608.
16. C. H. DRUMMOND III, W. E. LEE, W. A. SANDERS and J. D. KISER, *Proc. Ceram. Eng. Sci.* **9** (1988) 1343.
17. W. E. LEE, C. H. DRUMMOND III, G. E. HILMAS, J. D. KISER and W. A. SANDERS, *ibid.* **9** (1988) 1355.
18. S. KANG and J. H. SELVERIAN, *J. Mater. Sci.* **27** (1992) 45.

Received 3 July 1992

and accepted 3 February 1993